

AD-A129 478

EXPERIMENTAL STUDY OF RESONANCE RADIATION TRAPPING AS A 1/1
METHOD OF GAIN IM..(U) CALIFORNIA UNIV SAN DIEGO LA
JOLLA INST FOR PURE AND APPLIED P.. S LIN 30 SEP 81

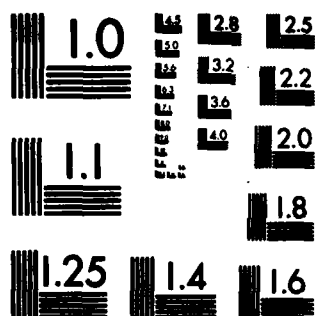
UNCLASSIFIED

N00014-80-C-0355

F/G 20/5

NL

END
DATE
FILMED
7 83
DTIC



MICROCOPY RESOLUTION TEST CHART
NATIONAL BUREAU OF STANDARDS-1963-A

DTIC FILE COPY

ADA129478

Experimental Study of Resonance Radiation Trapping as
a Method of Gain Improvement for Efficient Power
Extraction from the XeF Blue-Green Laser Transition

Shao-Chi Lin

University of California, San Diego

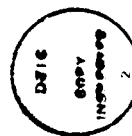
La Jolla, California 92093

Abstract

approximate
yield

An experimental study has been carried out to explore the possibility of utilizing resonance radiation trapping as a method of gain improvement for efficient power extraction from the XeF C - A blue-green laser transition. The experiment involved placing low-loss dichromatic mirrors to form a high-Q optical cavity around an x-ray preionized, homogeneous pulsed avalanche/self-sustained discharge of ~1 liter volume and ~200 nsec duration. The double-peak spectral reflectivity of the dichromatic mirrors was so chosen that most of the uv resonance radiation from the XeF B - X transition associated with the low-order TEM modes of the optical cavity could be trapped while the blue-green laser radiation built up within the same cavity from the C - A inversion could be partially coupled out. No gain improvement has been observed, however, in such an experiment. Instead, gain measurements at several XeF C - A transition wavelengths repeatedly showed large absorption losses during the early and late phases of the discharge, regardless of whether the uv resonance radiation trapping mirrors were used or not. Various factors which may have contributed to these negative results are examined and discussed.

A



Aviation Daily News	
Dist Special	
A	

I. INTRODUCTION

There appeared to have been considerable interests in the generation of visible lasers in the 470 - 510 nm wavelength region using the $C^2\Pi_{3/2} - A^2\Pi_{3/2}$ transition of the XeF excimer.¹⁻⁸ This transition is interesting not only because its emission spectrum happens to lie conveniently in the blue-green, but also because it is a bound-free transition so that the resultant laser action should be continuously tunable over the wavelength region just mentioned. Furthermore, very low population of the A-state is automatically guaranteed by the repulsive breakup of the XeF molecule immediately after the Franck-Condon transition. This tends to facilitate population inversion between the A- and C-states even at relatively low rates of excimer formation.

When the C-state excimer molecules are generated photolytically,⁵ the overall laser generation efficiency and output power can be expected to be ultimately limited by the efficiency and power of the photolytic light source, no matter how efficient is the subsequent process of excited states utilization. On the other hand, when the C-state is generated electrochemically in an e-beam or electric-discharge excited rare gas halogen mixture containing low mole fractions of Xe and F₂ or NF₃, past kinetics studies⁹ indicated that the total formation rate of the ionically bound XeF excited states can be expected to be proportional to the current density (or electron number density) and that the formation efficiency is generally very high. According to the spectroscopic studies of Kligler et al.¹ and Brashears et al.², the $C^2\Pi_{3/2}$ state was actually found to have a slightly lower (~ 0.08 eV) minimum potential energy than the $B^2\Sigma_{1/2}^+$ state, so that statistical equilibrium at or near room temperature

would favor a much higher (i. e., about a factor of 40) population of the $C^2\Pi_{3/2}$ state over that of the $B^2\Sigma_{1/2}^+$ state. However, during the main part of the e-beam or electric-discharge excitation pulse where both the mean electron energy and the electron number density remain high, the C- and B-states can be expected to be rapidly mixed and hence kept at nearly equal population density. At nearly equal C- and B-state population densities, the peak spectral gain of the C - A transition will always be much lower (by a factor of 50 - 100 at gas pressures of the order of 1 atm) than that of the B - X ultraviolet transition¹⁰ as long as this latter transition is not saturated. This is due to the much longer spontaneous emission lifetime¹¹ as well as the much wider emission bandwidth of the C - A bound-free transition in comparison with those of the B - X bound-bound transition. Because of this large disparity in spectral gain, it has been found necessary in the experiments reported by Fisher et al.⁶ and by Burnham⁸ to use anti-reflection coatings on the optical cavity mirrors in the 350 - 353 nm region in order to suppress the B - X laser oscillation. At the same time, the Q of the optical cavity was maximized in the 440 - 500 nm region to lower the laser oscillation threshold for the C - A transition. Even after such precautions, C - A laser oscillations were observed only toward the end of the excitation period or even in the after-glow on account of the slow intensity buildup associated with the small spectral gain. Because of the low cavity field intensity throughout the excitation period, the extractable laser power and pulse energy from the C - A transition were found to be very low when compared with what can be extracted from the B - X transition under identical excitation conditions. These led Fisher et al.⁶ to conclude that in order to realize the high

power, high efficiency potential of the tunable XeF C - A transition laser, a method would have to be found to saturate the C - A transition in order to compete effectively against the very rapid excited-state losses through the high-gain B - X transition. Burnham⁸ has estimated that if the B- and C-states are strongly coupled by electron collisions, efficient optical extraction of the C - A transition laser would require an intracavity flux of about 10 MW/cm^2 .

II. THE PROPOSED METHOD OF B - X RESONANCE RADIATION TRAPPING

As suggested in the original proposal which led to the present investigation,¹² one possible method for realizing the high power, high efficiency potential of the tunable XeF C - A transition laser is to do just the opposite of what has been done by the other investigators⁶⁻⁸ in regard to the treatment of the B - X uv radiation. That is, instead of minimizing the Q of the optical cavity to allow this uv radiation to escape as completely as possible to discourage B - X laser oscillations, it was proposed that the Q of the optical cavity be maximized so as to trap all the B - X resonance radiation¹³ as completely as possible. This can be done in principle, for example, through the use of a pair of low-loss dichromatic mirrors to form the optical cavity. The double-peaked spectral reflectivity is to be so chosen that the mirrors behave like perfect reflectors¹⁴ over the main part of the XeF B - X fluorescence spectrum (say, between 345 and 355 nm ¹⁰) and like good partial reflectors at the C - A transition wavelengths (470 - 510 nm). The transmittance of the partial reflectors,¹⁵ of course, must be properly matched to the spectral gain of the C - A transition for optimum blue-green laser output coupling. If so desired, dispersive elements (gratings, prisms, etc.) may also be added to the optical system to provide

tuning of the C → A laser oscillation and for selection of the laser output wave length.

To illustrate how trapping of the B → X resonance radiation may improve the small-signal (unsaturated) gain and hence facilitate power extraction from the C → A transition laser, let us refer to the symbolic energy level diagram shown in Fig. 1 and the dichromatic optical cavity mentioned in the preceding paragraph. Before the intracavity flux reaches the saturation intensity at either the B → X or the C → A transition frequencies, spontaneous emissions and amplified spontaneous emissions (ASE) will progress in the normal manner and the radiation patterns for these emissions will be nearly isotropic. In view of the fact that the optical cavity is open everywhere except at the mirror surfaces, and that the solid angles subtended by these mirrors from the excitation region are generally quite small, the usual assumption is that most of the spontaneous emission photons and ASE photons will escape. The rates of depletion of the B- and C-state populations per unit volume due to these processes are accordingly, n_B/τ_B and n_C/τ_C , respectively, where n_B and n_C denote the instantaneous number density of XeF excimer molecules in the B- and C-states, respectively, while τ_B and τ_C denote the corresponding spontaneous emission lifetimes for the two excited states. Here we have neglected the effects of ASE on the depletion rates of n_B and n_C . The neglect of ASE effect on n_C is certainly justifiable under marginal C → A gain conditions. The effect of ASE on n_B could be significant at the two ends of a long excitation volume under high gain conditions but is neglected here for consideration of the average depletion rate over the whole excitation volume during the early phases of the excitation

and gain buildup processes. As the excitation pulse progresses, laser oscillations will begin to build up. Due to the much higher gain of the B \rightarrow X transition mentioned earlier, laser oscillations from this transition can be expected to reach saturation intensities long before those arising from the C \rightarrow A transition. Since the Q of the cavity at the B \rightarrow X transition wavelengths is very high one may expect the field intensity at these wavelengths to reach very high saturation values. When this occurs, spontaneous emission may be suppressed and the B \rightarrow X radiation may become strongly trapped. This possibility is suggested by the early observation of Kluver¹⁶ that when a coherent signal of strong enough initial intensity to saturate the gain of the 3.508 μ m laser line was injected into a d.c. excited He-Xe discharge, the laser amplifier noise (i.e., amplified spontaneous emission) was greatly suppressed. Accordingly, for the purpose of a simple analysis, one may define a "trapping efficiency", to be denoted by the symbol η , for the B \rightarrow X radiation during the saturation period such that the net rate of depletion of the B-state population per unit volume due to the spontaneous emission process is reduced from n_B/τ_B to $(1 - \eta)n_B/\tau_B$. Even though the numerical value of η can only vary between 0 and 1 according to this definition, actual determination of its value on purely theoretical grounds can be quite complicated since the nonlinear effects of close coupling between the coherent radiation field and the molecular system must be taken into consideration.¹⁷ On the other hand, the effective value of η for any given saturated system can at least be determined, either directly or indirectly, through some suitable experimental arrangement. By making use of the trapping efficiency so defined and neglecting the rates of de-population of the excited states due to

stimulated emissions, one may then write down the rate equations governing the instantaneous number density of the B- and C-state excimer molecules:

$$\frac{dn_B}{dt} = R_B - (1 - \eta)n_B/\tau_B - k_{QB} n_M n_B, \quad (1)$$

$$\frac{dn_C}{dt} = R_C - n_C/\tau_C - k_{QC} n_M n_C, \quad (2)$$

where R_B and R_C denote the rate of formation of the XeF excimer molecules into the $B^2\Sigma_{1/2}^+$ and the $C^2\Pi_{3/2}$ state per unit volume per unit time, respectively, n_M denotes the total number density of all molecules in the gas mixture, and k_{QB} , k_{QC} denote the mixture-averaged collisional quenching rate coefficients for the B- and C-state molecules, respectively. It is important to note that when the B - X transition is already saturated, the B- and X-states are closely coupled by the intracavity field so that $n_B \approx n_X$. Thus, in neglecting the rate of depletion of the B-state molecules due to stimulated emission by the strong radiation field within the optical cavity, we are in effect assuming that the rate of removal of the XeF ground state molecules $X^2\Sigma_{1/2}^+$ by collisional dissociation (Fig. 1) is very slow in comparison with the rates of depletion of the B-state molecules due to the untrapped B - X spontaneous emission and due to collisional quenching.¹⁸ The neglect of the rate of depletion of the C-state population due to stimulated emission in Eq. (2) is, of course, completely justified since we are only considering the small-signal gain of the C - A transition at this point.

Assuming that the B- and C-states are very rapidly mixed by electron

collisions, one may let $n_B = n_C$, so that Eqs. (1) and (2) can be combined into a single equation,

$$2 \frac{dn_C}{dt} = R - [1 - \eta + (\tau_B/\tau_C) + \tau_B k_Q n_M] n_C / \tau_B, \quad (3)$$

where $R \equiv R_B + R_C$ represents the combined rate of formation of the B- and C-state excimer molecules, and $k_Q \equiv k_{QB} + k_{QC}$ represents the combined quenching rate coefficient for the B- and C-states. For quasi-steady-state excitations where $dn_C/dt \approx 0$, the C-state population density is given by

$$n_C = R \tau_B / [1 + (\tau_B/\tau_C) + \tau_B k_Q n_M - \eta]. \quad (4)$$

From this expression, one readily obtains the ratio of C-state population densities in the presence and in the absence of B \rightarrow X radiation trapping,

$$\frac{n_C(\eta)}{n_C(0)} = \frac{1 + (\tau_B/\tau_C) + \tau_B k_Q n_M}{1 + (\tau_B/\tau_C) + \tau_B k_Q n_M - \eta}. \quad (5)$$

Using the lifetime ratio $\tau_B/\tau_C = 1/6$ from Ref. 11, the numerical value of $n_C(\eta)/n_C(0)$ is plotted in Fig. 2 as a function of η for several values of the normalized collisional quenching rate, $\tau_B k_Q n_M$. For the typical He/Xe/NF₃ mixture cited in Refs. 6 and 8, and assuming that the combined collisional quenching rate for the B- and C-states by He is as negligible as what has been reported for quenching by Ne,¹⁹ the numerical value of $\tau_B k_Q n_M$ is typically of the order of 0.1. From Fig. 2, it is seen that if over 80% of the B \rightarrow X radiation can be trapped, a factor of 3 or 4 improvement on the C-state

population should be possible. Since the A-state population is always negligible due to the repulsive nature of the potential energy curve, the ratio $n_C(\eta)$ over $n_C(0)$ is also a direct measure of the improvement factor in spectral gain for the C - A transition due to trapping of the B - X radiation. It is important to note from Eq. (5) that the maximum improvement in the C-state population density, and hence the small-signal gain for the C - A transition, using the method of radiation trapping suggested here will be ultimately limited by the lifetime ratio $(\tau_B + \tau_C)/\tau_B = 7$. Nevertheless, from the point of view of power extraction and generation efficiency for the XeF visible laser, a factor of 3 or 4 improvement in small-signal gain would be very significant since the cavity buildup time is inversely proportional to the small signal gain. When such an improvement in small-signal gain is combined with homogeneous excitation using electron beams²⁰ or avalanche/self-sustained discharges of relatively large volumes and long pulse durations,^{21, 22} rapid gain saturation and efficient high-power extraction from the XeF C - A transition over a considerable part of its fluorescence spectrum should be quite possible.

III. EXPERIMENTAL APPARATUS AND EXPERIMENTAL ARRANGEMENTS

To test the idea of B - X radiation trapping as a possible method for improving the small-signal gain of the XeF C - A transition as outlined in the preceding section, we have carried out a number of exploratory experiments using the rare gas halide excimer laser research facility which has already been successfully developed at UC San Diego under previous DARPA/ONR fundings.²³ As illustrated in Figs. 3 through 8, this facility consists of a low-

inductance discharge apparatus with a water-dielectric pulse forming network (PFN); an x-ray preionization source driven by a high-voltage, high current electron beam which can also be used for direct pumping of the laser gas mixture or for sustaining a sub-avalanche discharge; a halogen gas handling system; a low-inductance rail gap switch for pulse sharpening; high-voltage generators; and various timing and triggering circuits. The discharge chamber has a maximum useable discharge volume of approximately 6 liters. It was constructed from stainless steel, aluminum, teflon, and kynar (polyvinylidene) and is, therefore, halogen-compatible. The particular geometries of the laser chamber, rail gap switch, and high voltage feedthroughs were so arranged that the nominal PFN characteristic impedance is maintained all the way up to the electrical interface of the PFN and the laser chamber. The electrical feedthroughs consisted of two 0.63 cm x 56 cm rounded-edges aluminum plates in order to provide a very low inductance high voltage connector. The total unmatched circuit inductance is only due to the discharge volume itself and was estimated to be less than 40 nH. The water-dielectric PFN is essentially a double-parallel-plate transmission line. This transmission line PFN was designed and constructed in modular form consisting of 100 nsec sections. The PFN can be operated at voltages ranging from 20 to 150 kV at a characteristic impedance of a few ohms down to about 1/4 ohm, even though the nominal impedance has been fixed at 0.5 ohm for most of the experiments performed so far.^{21, 22}

Using the above described apparatus in the x-ray preionized pulsed avalanche/self-sustained discharge mode, we have succeeded in generating

very homogeneous pulsed avalanche discharges of about 2.5 liter volume at 1 atm pressure in rare gas/halogen mixtures containing typically 0.2% halogen over a pulse duration of about 100 nsec. This is illustrated in Figs. 9a and 9c which show a Polaroid photograph of the homogeneous plasma luminosity from the x-ray preionized discharge and the corresponding uniform uv laser burn pattern on a piece of developed Polaroid film mounted 1 m away from the output mirror. The laser pulse energy output from the 100 nsec discharge was typically 2.5 J for XeCl, 1.4 J for KrF, and 0.25 J for XeF.²¹

The experimental arrangement for measuring the spectral gain in the blue-green region corresponding to the $\text{XeF } C^2\Pi_{3/2} \rightarrow A^2\Pi_{3/2}$ transition is illustrated schematically in Fig. 10. The probe laser employed is a TRW Model 71B pulsed argon ion laser of approximately 1 μsec pulse duration FWHM (Full Width at Half-Maximum intensity) and 1 W peak power. As is well known, a free-running argon ion laser with broad-band cavity mirrors shows many strong lines within the XeF C \rightarrow A emission spectrum. These lines, the strongest of which are located at $\lambda = 472.69, 476.49, 487.99, 496.51, 501.72,$ and 514.53 nm , respectively, can easily be separated by a dispersive element (prism). All these lines have been utilized in our gain measurement but the results are found to be essentially similar and show no significant wavelength dependence.

After wavelength selection through the prism (Fig. 10), the argon ion laser probe beam is double-passed through the gain medium generated in the x-ray preionized discharge chamber using dielectric coated mirrors. The amplified (or attenuated) probe beam emerging from the discharge chamber

is then directed through a number of collimating lenses and filters and finally onto an ITT biplanar photodiode inside a screen cage. A number of limiting apertures are also used in addition to the uv filters to minimize collection of the strong $\text{XeF } B^2\Sigma - X^2\Sigma$ spontaneous emission by the broad-band photodiode detector. The photo-detector output is displayed on a Tektronix 7104 oscilloscope* inside the screen cage and recorded on Polaroid film. Triggering of the pulsed argon ion laser and of the x-ray preionized discharge is properly synchronized by time-delayed pulse generators so that the discharge pulse of 100 nsec duration always occur near the peak of the argon ion laser pulse of 1 μ sec FWHM duration.

For generation of the XeF excimers in the discharge chamber, Xe/NF_3 and Xe/F_2 mixtures are used with either He or Ne as the diluent gas. Many different mixture ratios have been tried, with the Xe concentration generally in the range of 0.1 to 2 mol percent and NF_3 or F_2 varying between 0.05 and 0.5 mol percent. The total initial gas pressure is in the range of 1 to 2.6 atm (15 to 38 psia). In all the experiments, the effective length of the discharge electrodes is fixed at 110 cm (double-pass gain length = 220 cm). The effective width of the electrodes is kept constant at 3 cm, and the gap spacing between anode and cathode is also fixed at 3 cm so that the effective excitation volume is approximately 1 liter. The discharge chamber is provided with anti-reflection coated fused silica windows at both ends for good transmission at both uv and visible wavelengths. For gain measurements

* Due to a persistent lack of fund for updating of instrumentation at the University, the generous help of Tektronix, Inc., San Diego office, in providing us a demonstrator model 7104 oscilloscope on temporary loan for carrying out these experiments are hereby gratefully acknowledge.

without trapping of the XeF B - X resonance radiation, no optical cavity mirrors are used at either end of the discharge chamber. For gain measurements with trapping of the XeF B - X resonance radiation, a pair of dielectric-coated uv mirrors of approximately 98% maximum reflectance at $\lambda = 351$ nm and 90% transmittance at the blue-green ($470 < \lambda < 510$ nm) are mounted internally to replace the discharge chamber end windows and aligned with the optical axis of the out-going probe beam. These mirrors are of 2-inch diameter, 5-meter concave radius of curvature, and coated on fused silica substrates by the CVI Corporation. For observation of the XeF C - A laser oscillation in the blue-green in the presence of B - X resonance radiation trapping, the argon ion laser probe beam is turned off and the uv mirrors are replaced by a pair of dichromatic mirrors of 2-inch diameter and 5-meter concave radius of curvature. The dichromatic mirrors, also supplied by the CVI Corporation, are rated at 96 - 98% maximum reflectance and 0.5 - 1% transmittance at both the uv and blue-green wavelengths (i. e., $\lambda \approx 351$ and 488 nm, respectively).

In addition to the gain measurements and laser oscillation experiments, comparison of the spontaneous emission intensities of the XeF B - X radiation in the direction perpendicular to the optical axis of the laser oscillator cavity in the absence and in the presence of B - X resonance radiation trapping has also been made. These "side-light fluorescence" experiments were made inside the discharge chamber using a quartz fiber bundle of 0.25 numerical aperture directed across the discharge gap from the side-wall teflon insulator. The B - X uv radiation collected by the small quartz prism at the input end of the fiber bundle is guided out of the discharge chamber through one of its

end walls. The light output is then filtered by an interference filter of 12-nm bandwidth (FWHM) and detected by an EMI 9781B photomultiplier tube. The output from the latter is amplified by a Mini-Circuits ZHL-32A amplifier of 150 MHz bandwidth and displayed on a Tektronix 519 oscilloscope.

IV. EXPERIMENTAL RESULTS*

1. Gain Measurements

Gain measurements in the blue-green region corresponding to the XeF $C^2\Pi_{3/2} - A^2\Pi_{3/2}$ transition using the experimental arrangement described in the preceding section (Fig. 10) have been carried out with the electrical length (2-way wave propagation time) of the water-dielectric transmission line which drives the pulsed avalanche discharge (Fig. 7) set at 100 and 200 nsec., respectively, in two distinct sequences of experiments. The two sequences were separated by a substantial period of time (~ 6 months) necessitated by all the mechanical and electrical works entailed. No significant difference in results is observed, however, in these two sequences of experiments in spite of a factor-of-2 difference in total discharge time. This suggests that the time variations of absorption and gain at the XeF C - A transition wavelengths are probably governed by secondary rate processes not directly correlated with the instantaneous electron number density in the long duration pulsed discharges.

In Fig. 11, we show some typical oscillographic traces of the XeF C - A gain (or absorption) signal observed in the 200 nsec discharge experiments.

*The experimental results presented here represent the collective works done by former graduate students Jeffrey I. Levatter, Yuh-Shuh Wang, and Karin L. Robertson during the 21-month performance period, 1/1/80 - 9/30/81.

The gas mixture employed here is of initial mol ratio $\text{He}:\text{Xe}:\text{NF}_3 = 996:3:1$ and the total gas pressure p is 1 and 2.4 atm for the traces on the left and right columns, respectively. The pulse-charged voltage on the transmission line, which is initially isolated from the discharge chamber before rail gap switching (Fig. 6), is ~ 50 kV. From the lower traces, it is seen that the discharge voltage across the electrodes first rises rapidly upon rail gap switching, reaching a peak of ~ 50 kV, and then drops rapidly as the avalanche process approaches completion at $t \sim 20$ or 30 nsec, depending on the gas pressure. The discharge voltage is then stably self-sustained at a level which is roughly proportional to the gas pressure until the end of the ~ 200 nsec period. The voltage waveform is, therefore, very similar to those observed in the XeCl laser discharge reported in Ref. 22. The gain coefficient plotted in Fig. 12, which is deduced directly from the transmitted probe beam intensity shown in the upper traces of Fig. 11 and from the known pulse shape of the probe laser power output assuming a linear photodiode response, however, indicate that the spectral gain of the excited plasma at the probe beam wavelength $\lambda = 487.99$ nm is first negative (i. e., positive absorption) during the avalanche phase of the discharge. It remains negative for a period of time which appears to vary inversely with the total gas pressure p (i. e., $10 < t < 85$ nsec at $p = 1$ atm, and $10 < t < 65$ nsec at $p = 2.4$ atm, where $t = 0$ refers to the instant of rail gap switching). After this period, the gain becomes positive over a time duration which is again varying inversely with the total gas pressure ($85 < t < 220$ nsec at $p = 1$ atm, and $65 < t < 120$ nsec at $p = 2.4$ atm). At later times, the gain returns to a negative value for the remain-

der of the observation period (500 nsec) and such negative value appears to be a rapidly increasing function of the gas pressure.

In Fig. 13, we show a plot of the time variations of the spectral absorption and gain observed in the 100 nsec discharge experiments using a somewhat different mixture mol ratio ($\text{He}:\text{Xe}:\text{NF}_3 = 9986:8:6$) at three different values of the initial total gas pressure, $p = 1, 1.7$, and 2.5 atm. These are deduced from oscillographic traces of the transmitted probe beam intensity similar to those shown in Fig. 11 when the electrical length of the transmission line (Fig. 6) was set at 100 nsec. The probe beam wavelength is again 487.99 nm. As in the case of the XeCl laser discharge experiments reported in Ref. 22, the discharge voltage waveforms are also quite similar to those shown in the lower traces of Fig. 11 except for an earlier termination of the nearly flat self-sustaining voltage plateau at $t \sim 100$ nsec instead of 200 nsec. Comparing Figs. 12 and 13, it is seen that the overall pressure dependence and absolute values of the peak absorption and gain coefficients observed in the two sets of experiments are surprisingly similar in spite of the difference in initial mixture mol ratio and the factor-of-2 difference in total discharge time. In fact, the general waveform of the transmitted beam intensity showing the initial absorption, subsequent positive gain, and late time absorption is quite similar to those observed by Fisher et al.⁶ in their uv preionized discharge experiments of 40 nsec FWHM current pulse duration in a $\text{He}:\text{Xe}:\text{NF}_3 = 2280:3:2$ mixture at $p = 3$ atm. The initial absorption and subsequent gain were also observed by Hill et al.²⁴ in their e-beam-excited $\text{Ar}:\text{Xe}:\text{NF}_3 = 12160:3:10$ mixture at $p = 16$ atm over a total observation period of ~ 100 nsec.

The highest positive gain observed in our experiments is from the mixture of initial mol ratio $\text{He}:\text{Xe}:\text{NF}_3 = 996:3:1$ at a total gas pressure of 2.4 atm (Fig. 12). Unfortunately, this mixture mol ratio and total gas pressure also yielded the shortest period of positive gain and the highest late-time absorption among all the mixtures and gas pressures tested. The peak gain coefficient observed here, $g_{\text{max}} \approx 2 \times 10^{-3} \text{ cm}^{-1}$, is comparable to, but somewhat lower than that reported by Fisher et al. in Ref. 6. In varying the mole ratio of the $\text{He}/\text{Xe}/\text{NF}_3$ mixture, it is found that there is no dramatic change in the time variation of the spectral gain except when the Xe mol fraction is markedly increased. Thus, at the mol ratio $\text{He}:\text{Xe}:\text{NF}_3 = 979:20:1$, positive gain is observed only at $p = 1$ atm and at no other pressure. The use of F_2 in place of NF_3 as the fluorine donor makes both the gain and absorption levels less sensitive to changes in gas pressure, but the gain is relatively low in comparison with that obtained from the NF_3 mixtures.

The early-time absorption observed in our experiments and in the experiments reported in Refs. 6 and 24 are most likely caused by some higher-lying excited states of Xe or by photodetachment of F^- even though no positive identification has yet been made. [Note that the same early-time absorption have been observed at many different probe beam wavelengths in the blue-green so that the absorption must be broad-band. On the other hand, the blue-green wavelengths are all below the threshold energy for photoionization of the lower-lying Xe metastables. The absorption spectra of some of the molecular species, such as Xe_2^+ and Xe_2^* , may also extend into the blue-green, but the formation rates of these species are probably too low to make these species

significant contributors to the early-time absorption.] Continuous production of these absorbing species during the XeF excimer formation period may well be a major limiting factor of the spectral gain at the C - A transition wavelengths.

In regard to the late-time absorption observed after the positive gain period, Fisher et al.⁶ suggested that this is a beam steering effect due to the buildup of transverse refractive index gradient rather than molecular absorption. However, we find that when binary mixtures of He/Xe and He/F₂ are used in place of the He/Xe/NF₃ mixture in our discharge experiments, no absorption nor gain is observed at the same blue-green probe beam wavelengths. The absence of beam steering effects here is probably due to the fact that the transverse dimensions of our discharge plasma (~ 3 cm) is much greater than the diameter of the Ar⁺ laser probe beam employed (~ 0.3 cm). On the other hand, when the binary mixture He/NF₃ is used in our discharge, late-time absorption of magnitude comparable to that observed in the He/Xe/NF₃ mixture is again observed, even though there is no positive gain. This indicates that the late-time absorption observed in our experiments must be of a molecular nature. In fact, it may well be caused by some decomposed fragments of NF₃ (e.g., NF₂, NF, etc.) even though no positive identification has yet been made.

In Fig. 14, we show a comparison of the time variations of the spectral absorption and gain observed at $\lambda = 487.99$ nm in the absence and in the presence of B - X resonance radiation trapping. The gas mixture employed here is He:Xe:NF₃ = 9986:8:6 at $p = 1$ atm, and the discharge pulse duration is

100 nsec. The solid curve is obtained from the gain measurement without using any uv cavity mirrors for trapping the XeF B - X resonance radiation and is, therefore, the same as the $p = 1$ atm curve shown in Fig. 13. The dotted curve shown in Fig. 14, on the other hand, is obtained by directing the once-reflected Ar^+ laser probe beam (Fig. 10) through a pair of pre-aligned uv cavity mirrors of $\sim 98\%$ maximum reflectance at $\lambda = 351$ nm, $\sim 90\%$ transmittance at $\lambda = 487.99$ nm, 2-inch diameter, and 5-meter concave radius of curvature as described earlier in Section III. It is seen that the two curves are identical during the early absorption period and departs from each other by about 20% during the subsequent positive gain period, with the uv trapping curve showing a lower gain. During the late-time absorption period, the two curves show greater departure ($\sim 40\%$), with the uv trapping curve showing a smaller absorption. Experiments with other He:Xe:NF₃ mol ratios and total gas pressures show similar trends. In no case have we yet observed a spectral gain that is higher with uv resonance radiation trapping than without uv resonance radiation trapping at the XeF C - A transition wavelengths.

2. Laser Oscillation Experiments

Laser oscillation experiments at the XeF C - A transition wavelengths have been performed using the stable resonator cavity formed by the dichromatic mirrors within which the XeF B - X resonance radiation is intentionally trapped. As described in Section III, these mirrors are of 2-inch diameter, 5-meter concave radius of curvature, and dielectric-coated on fused silica substrates by the CVI Corporation. According to the specifications provided by CVI, these mirrors are rated at 96 - 98% maximum reflectance and 0.5 -

1% transmittance at both the uv and the blue-green wavelengths (i. e., at $\lambda = 351$ and 488 nm, respectively) and were coated according to the best available technology at the time when the mirrors were ordered. The peak reflectance at $\lambda \approx 351$ nm is intended for trapping of the B \rightarrow X resonance radiation as much as possible while the peak reflectance at $\lambda \approx 488$ nm is intended for building up the C \rightarrow A laser oscillation within a high-Q resonator cavity of small but finite output coupling coefficient. The mirrors are internally mounted to replace the end windows of the discharge chamber so as to maximize the Q of the optical cavity at the two selected wavelengths. The mirrors are pre-aligned before each discharge, using the Ar^+ probe laser. The probe laser is turned off before initiation of the pulsed avalanche discharge. Laser oscillation at the blue-green wavelengths, if any, is detected by the same photodiode used in the spectral gain and absorption experiments (Fig. 10).

The results of the XeF C \rightarrow A laser oscillation experiments just described have been completely negative, in the sense that no laser power output above the noise level has been observed using the same set of gas mixtures and over the same range of discharge conditions as described in the spectral gain and absorption experiments. Since the Ar^+ probe laser is turned off during the discharge, these experiments can be considered as self-excited laser oscillation experiments in the absence of any injected signal.

In addition to the self-excited laser oscillation experiment just mentioned, we have also performed some C \rightarrow A laser oscillation experiments with narrow-band signal injection. This is accomplished simply by leaving the Ar^+ probe laser on during the pulsed discharge. In this case, the pulsed avalanche dis-

charge is synchronously triggered with the pulsed Ar^+ probe laser so that the discharge takes place during the period of maximum probe laser intensity. With a maximum transmittance of 0.5 - 1% for the cavity mirrors and a maximum Ar^+ laser power of about 0.4 W at $\lambda = 487.99$ nm in the probe beam of ~ 0.3 cm diameter, the injected beam power density into the optical cavity is, therefore, of the order of $3 \times 10^{-2} \text{ W/cm}^2$. The $\text{XeF C} \rightarrow \text{A}$ laser oscillator power output, if any, is detected together with the transmitted power of the Ar^+ laser probe beam through the optical cavity by the same photodiode. In view of the fact that the experimental arrangement here is actually identical to that of the spectral gain and absorption experiments described earlier in Section III and Sub-section IV-1, the laser oscillation experiment with narrow-band signal injection can also be considered as a spectral gain and absorption measurement at the $\text{XeF C} \rightarrow \text{A}$ transition wavelengths in the presence of $\text{B} \rightarrow \text{X}$ resonance radiation trapping within the dichromatic optical cavity.

In Fig. 15, we show some typical oscillographic traces of the Ar^+ laser probe beam signal at $\lambda = 487.99$ nm through the dichromatic optical cavity during the x-ray preionized pulsed avalanche discharge in the presence of $\text{XeF B} \rightarrow \text{X}$ resonance radiation trapping under otherwise identical experimental conditions as in the simple gain and absorption experiment illustrated in Fig. 11. As in Fig. 11, the initial offset of the oscillographic trace is so arranged that the zero-level of detected probe beam intensity is aligned with the bottom line of the oscillogram. Thus, the instantaneous gain or absorption can be inferred from the vertical position of the oscillographic trace relative to that observed before the avalanche discharge is initiated near $t = 0$. However, in contrast

to the simple gain and absorption measurement where the effective path length is simply twice the length of the discharge gas sample, the effective total propagation path length here is determined by the Q of the optical cavity as well as by the length of the excited gas sample. Nevertheless, the relative magnitudes of the peak gain and of the maximum absorption during each discharge can readily be compared through the corresponding maximum upward and downward deflections of the oscillographic trace from the initial vertical position. Comparing the upper row of oscillographic traces shown in Fig. 15 with that shown in Fig. 11, it is seen that the observed peak gain in the presence of XeF B \rightarrow X resonance radiation trapping is considerably lower than that observed in the absence of B \rightarrow X resonance radiation trapping. When viewed as a XeF C \rightarrow A laser oscillation experiment with narrow-band signal injection, the smallness of the incremental total detected power by the photodiode during the peak gain period observed here indicates that the C \rightarrow A laser oscillator output, if any, is below the noise level.

3. Side-Light Fluorescence

The side-light fluorescence measurements (Section III) show a slight suppression of the XeF B \rightarrow X and C \rightarrow A spontaneous emission intensity when the end windows of the discharge chamber are replaced by the monochromatic uv cavity mirrors or by the dichromatic uv and blue-green cavity mirrors. The amount of suppression is only comparable to that of the suppression of peak gain shown in Fig. 14. The time-variations of the XeF B \rightarrow X side-light fluorescence is qualitatively similar to that reported in Ref. 22 for the XeCl B \rightarrow X transition.

V. DISCUSSIONS

The negative experimental results observed in the present investigation suggest that the XeF B - X resonance radiation "trapping efficiency", η , as defined in our theoretical model (Section II and Fig. 2) that can be achieved using the available optical components is exceedingly low. In fact, the trapping effect is generally so weak that it is not sufficient to overcome the factor-of-2 suppression of the B-state population which is to be expected during a sudden gain-switching of the B - X transition. In our theoretical model, we implicitly assumed that gain-switching is a relatively short transient in a relatively long quasi-steady-state discharge. Thus, in our analytical model, we assumed that in the quasi-steady-state period under consideration, the B - X transition is already optically saturated after gain-switching, and the B- and X-states are closely coupled by the strong intracavity field so that $n_B \approx n_X$. Furthermore, it was assumed that the B- and C-states are rapidly mixed by the free electrons and that the rate of removal of the weakly-bound $X^2\Sigma_{1/2}^+$ ground electronic state by collisional dissociation (Fig. 1) is very slow. Thus, even though the C-state population may be momentarily depressed together with the B-state population during the B - X gain-switching, one may expect a rather rapid recovery and eventual increase of the combined B- and C-state population beyond the pre-gain-switching level. This would be the case, for example, if the kinetic rates of production of the B- and C-states remain very high in comparison with the total loss rate of the B- and X-states due to incomplete resonance radiation trapping and collisional dissociation after gain-switching. Since this expected rapid recovery and subsequent improvement of the

C - A small-signal gain have not been observed in any of our long duration (up to 200 nsec) pulsed discharge experiments, we may tentatively conclude that the transient effect of B - X gain-switching cannot be ignored, or that some of the requirements for satisfying the various inequalities in time scales assumed in our quasi-steady-state model cannot be met under our experimental conditions. In order to gain a better understanding of this problem, however, one must carry out a more detailed kinetics study of the XeF laser discharge, gain-switching, and other transient rate processes in a manner similar to what has recently been carried out for the XeCl laser discharge.²⁵

Another surprising result of the present investigation is the apparent predominance of the spectral absorption over gain during most of the observation period and at all the Ar^+ laser probe beam wavelengths tested. In fact, the onset time, peak value, and FWHM duration of the positive gain period at the XeF C - A transition wavelengths observed at a fixed mixture mol ratio and total gas pressure appear to be quite independent of whether the discharge pulse duration is 100 or 200 nsec (Sub-section IV-1). The duration of the positive gain period also tends to decrease with increasing gas pressure and peak gain. With such predominance of absorption and only a brief appearance of positive gain, no matter how long the discharge current pulse, building up of the C - A blue-green laser modes within the optical cavity would be quite difficult. Accordingly, better understanding of such strong absorption effect, and discovery of methods toward its elimination, are just as important as reduction of the depletion rates of the B- and C-state populations due to spontaneous emission for further improvement of the XeF C - A laser performance.

REFERENCES AND FOOTNOTES

1. D. Kligler, H. H. Nakano, D. L. Huestis, W. K. Bischel, R. M. Hill, and C. K. Rhodes, *Appl. Phys. Lett.* 33, 39 (1978).
2. H. C. Brashears, Jr. and D. W. Setser, *Appl. Phys. Lett.* 33, 821 (1978).
3. C. H. Fisher and R. E. Center, *J. Chem. Phys.* 69, 2011 (1978).
4. T. G. Finn, L. J. Palumbo and L. F. Champagne, *Appl. Phys. Lett.* 34, 52 (1979).
5. W. K. Bischel, H. H. Nakano, D. J. Eckstrom, R. M. Hill, D. L. Huestis, and D. C. Lorents, *Appl. Phys. Lett.* 34, 565 (1979).
6. C. H. Fisher, R. E. Center, G. J. Mullaney and J. P. McDaniel, *Appl. Phys. Lett.* 35, 26 (1979).
7. W. E. Ernst and F. K. Tittel, *Appl. Phys. Lett.* 35, 36 (1979).
8. R. Burnham, *Appl. Phys. Lett.* 35, 48 (1979).
9. C. A. Brau, Rare Gas Halogen Excimers (Chapter 4 in Excimer Lasers, edited by C. K. Rhodes, Springer-Verlag, Berlin Heidelberg New York, 1979), p. 87.
10. C. A. Brau and J. J. Ewing, *J. Chem. Phys.* 63, 4640 (1975).
11. R. W. Waynant and J. G. Eden, *IEEE J. Quantum Electron.* QE-15, 61 (1979).
12. The B - X radiation can be considered as "resonance radiation" since it connects to the ground electronic state $X^2\Sigma_{1/2}^+$, even though the vibrational-rotational levels directly involved in the optical transition may not at all be the lowest energy levels due to the Franck-Condon selection as noted in Refs. 10 and 13.
13. J. Tellinghuisen, G. C. Tisone, J. M. Hoffman, and A. K. Hays, *J. Chem. Phys.* 64, 4796 (1976).
14. Or, more realistically, like "nearly perfect" reflectors, after some allowance is made for the inevitable absorption and scattering losses in the dielectric coatings.

15. Obviously, in any asymmetric optical cavity arrangement, only one of the two mirrors needs to be a partial reflector for output coupling at the XeF C - A laser oscillation wavelengths.
16. J. W. Kluver, J. Appl. Phys. 37, 2987 (1966).
17. W. E. Lamb, Jr., Phys. Rev. 134, A1429 (1964).
18. In contrast to the problem of power extraction from the XeF uv laser where a high rate of removal of the XeF ground state molecules, $X^2\Sigma_{1/2}^+$, is desirable (Ref. 20), a very slow rate of removal of these ground state excimer molecules is needed here for trapping of the B - X resonance radiation. Accordingly, lowering the gas temperature would be helpful in this case.
19. M. Rokni, J. H. Jacob, J. A. Mangano, and R. Brochu, Appl. Phys. Lett. 32, 223 (1978).
20. J. C. Hsia, J. A. Mangano, J. H. Jacob, and M. Rokni, Appl. Phys. Lett. 34, 208 (1979).
21. S. C. Lin and J. I. Levatter, Appl. Phys. Lett. 34, 505 (1979).
22. J. I. Levatter, K. L. Robertson, and S. C. Lin, Appl. Phys. Lett. 39, 297 (1981).
23. S. C. Lin, "X-Ray Preionization for Excimer Laser Generation," University of California, San Diego, Proposal No. UCSD-9862 submitted to the Office of Naval Research April 1, 1977 and funded September 1, 1977. Actually, a proposal to explore the same idea of X-ray preionization for homogeneous initiation of pulsed avalanche discharges was submitted to the Defense Advanced Research Projects Agency as early as 1974 by the Principal Investigator, but no serious work was started at that time due to a lack of funding support.
24. R. M. Hill, P. L. Trevor, D. L. Huestis, and D. C. Lorents, Appl. Phys. Lett. 34, 137 (1979).
25. Y. S. Wang, "A Theoretical Study of the Kinetic Processes in a High-Power Xenon Chloride Excimer Laser Oscillator Driven by a Long Transmission Line Pulse Forming Network," Ph. D. Dissertation, University of California, San Diego (1982).

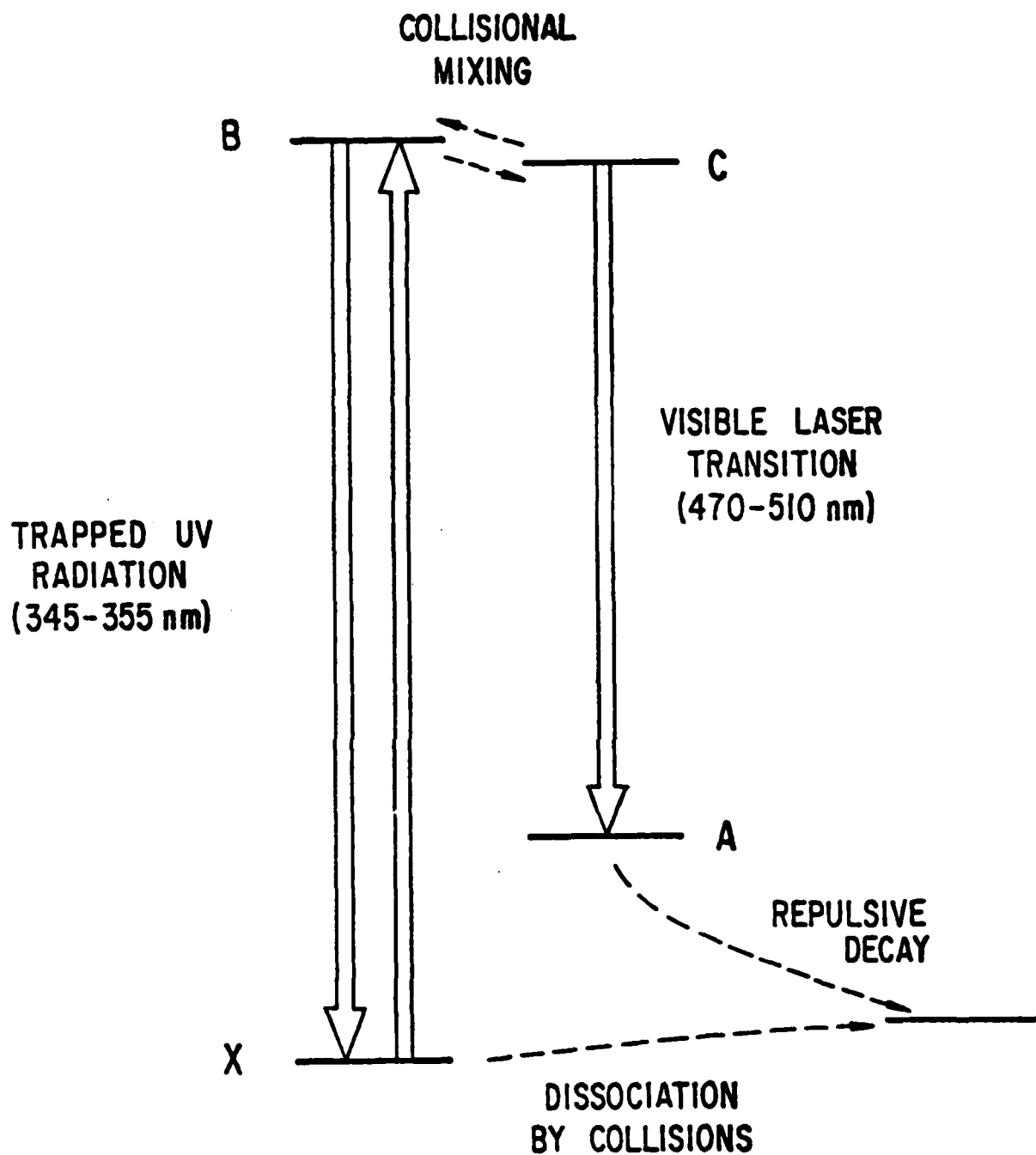


Fig. 1. Symbolic energy level diagram showing the various physical processes associated with the proposed method for enhancing the small-signal gain of the XeF $C \rightarrow A$ visible laser transition through trapping of the $B \rightarrow X$ uv resonance radiation.

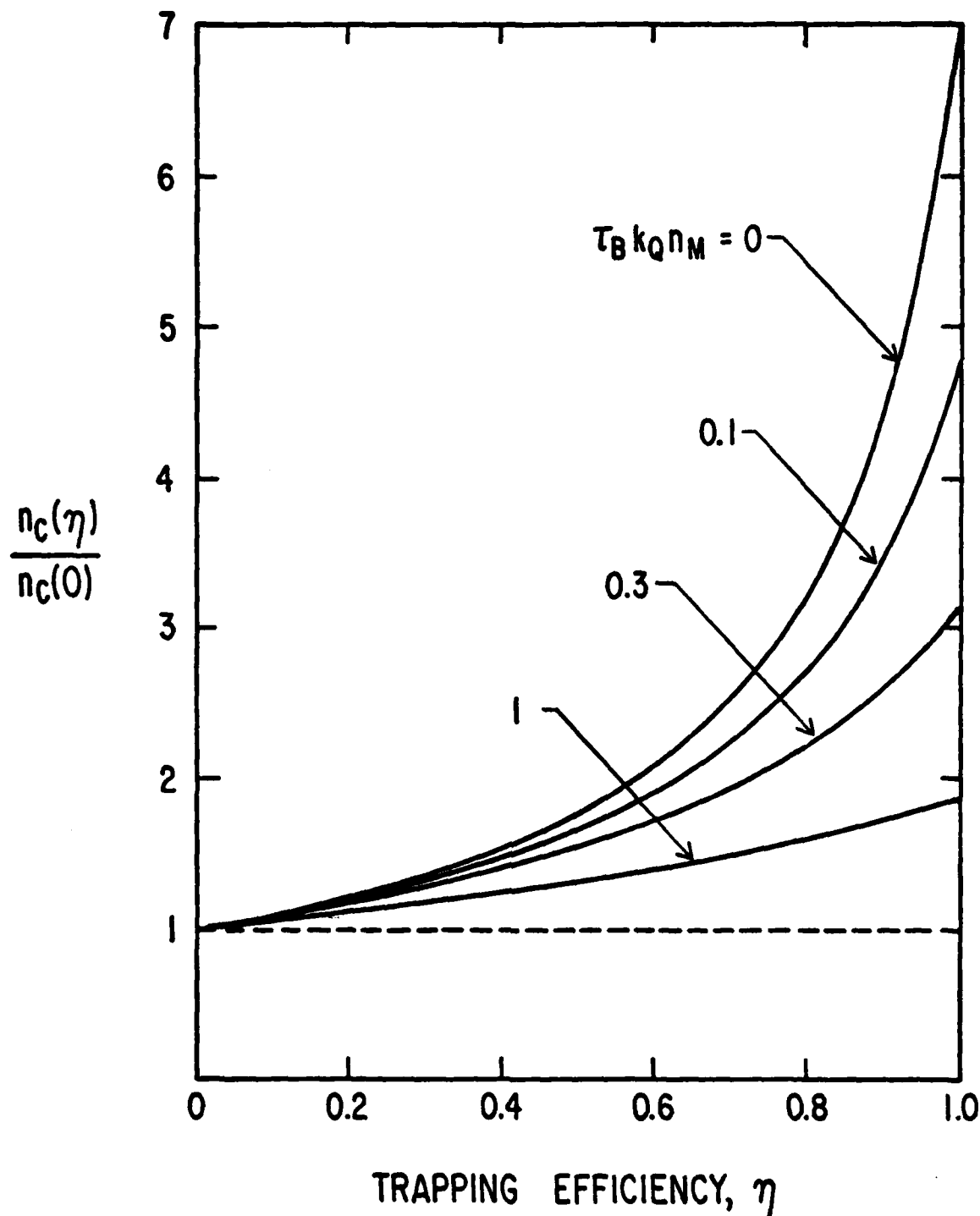


Fig. 2. Ratio of the XeF C-state population densities in the presence and in the absence of $B \rightarrow X$ radiation trapping as a function of the trapping efficiency, η , at various selected values of the normalized collisional quenching rate, $\tau_B k_Q n_M$. It may be noted that this ratio is nearly identical to the inversion density ratio and the small-signal gain ratio for the $C \rightarrow A$ transition in the presence and in the absence of $B \rightarrow X$ radiation trapping since the population density for the repulsive A-state is always negligible.

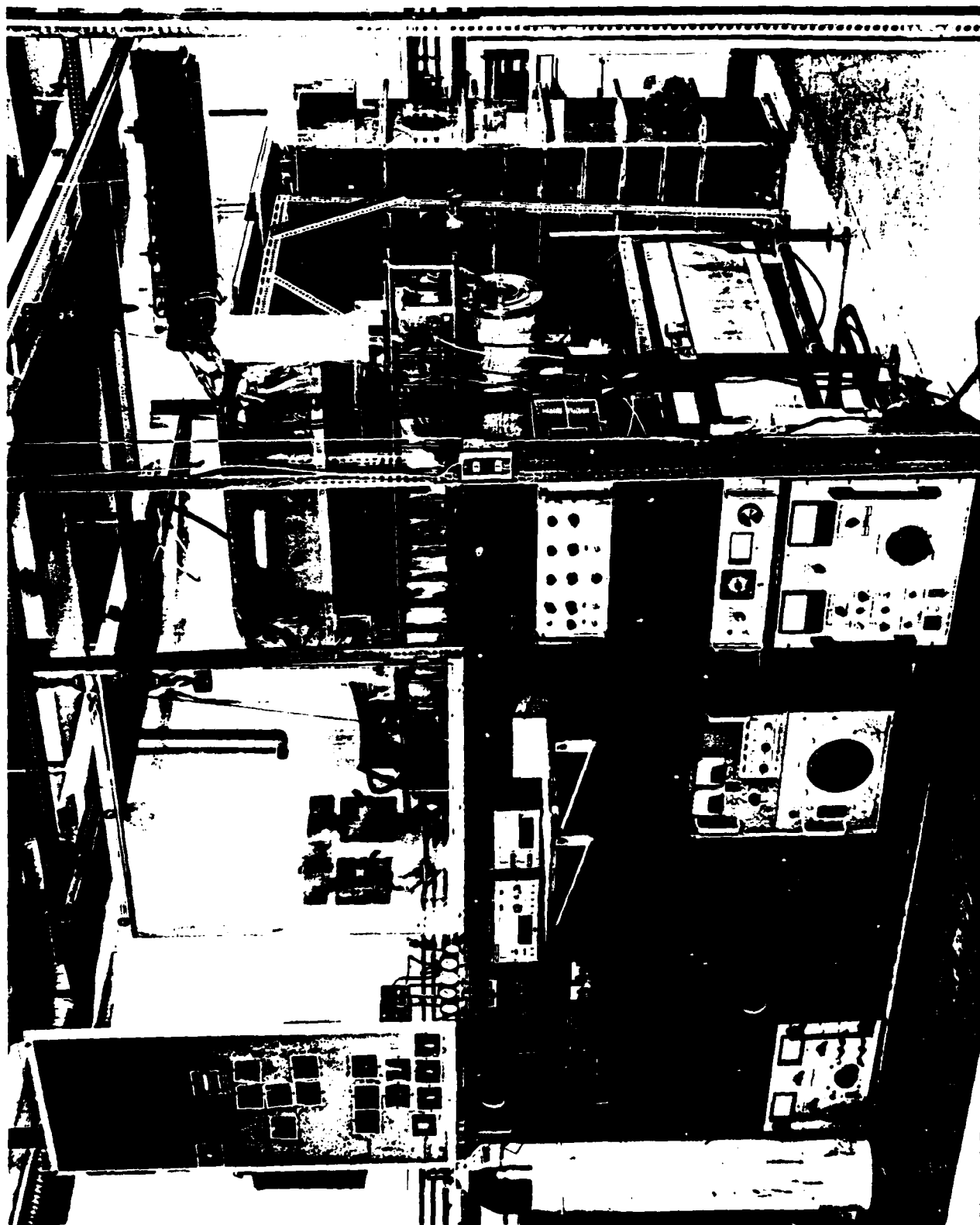


Fig. 3. Photograph of the low inductance discharge apparatus with transmission line drive and x-ray preionization provisions.

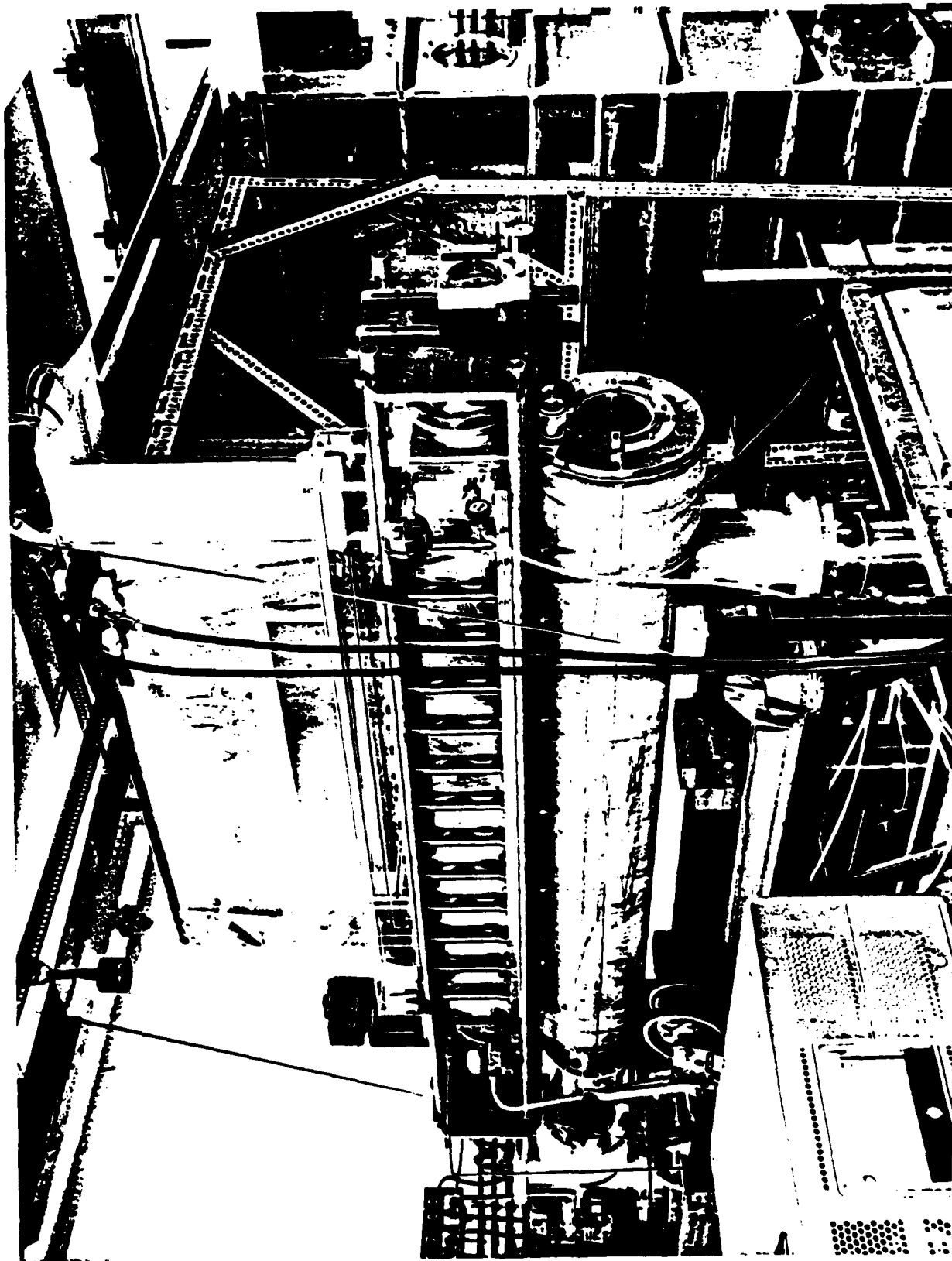


Fig. 4. Photograph of the multi-liter-volume, x-ray preionized, pulsed avalanche/self-sustained discharge apparatus at UC San Diego.

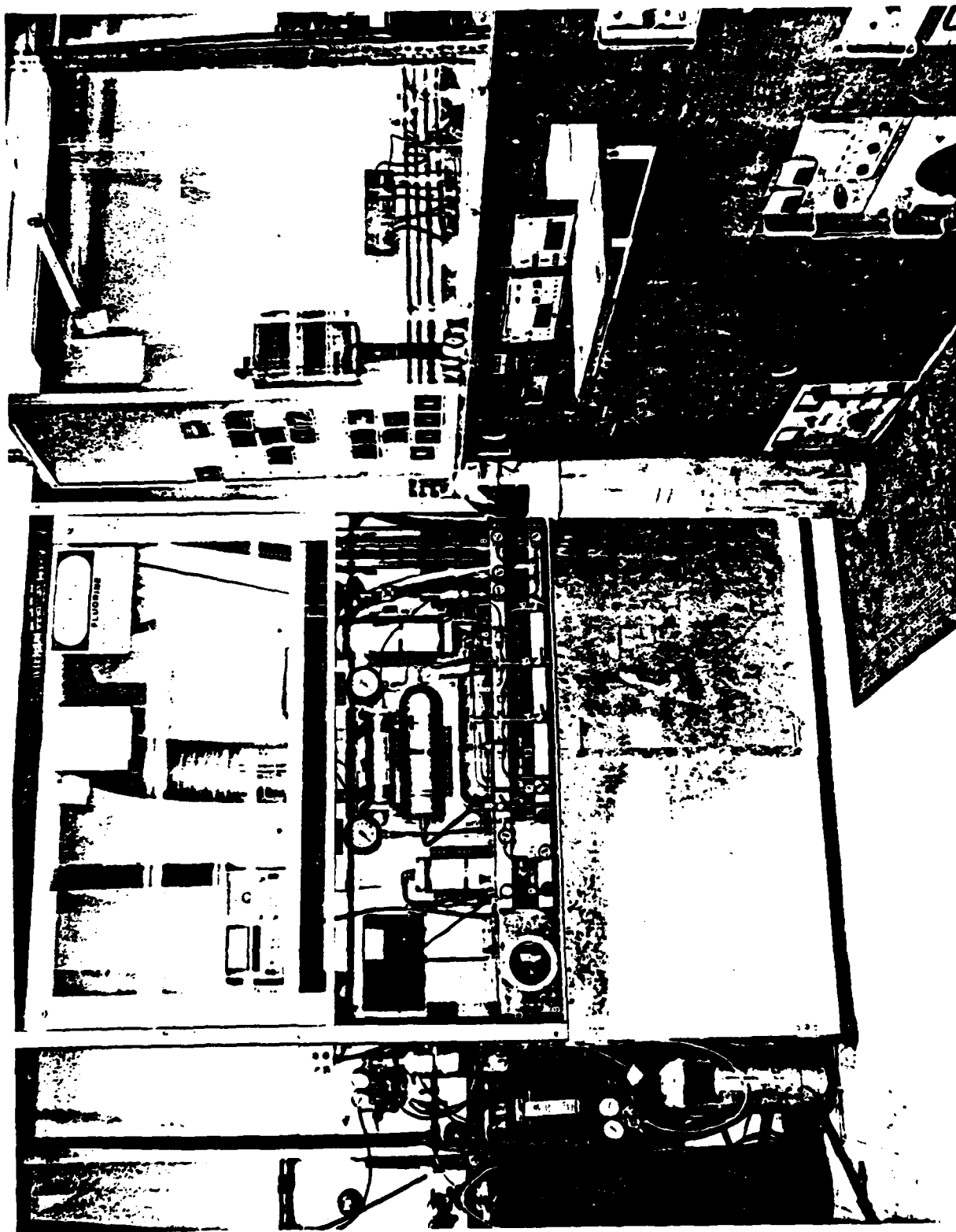


Fig. 5. Gas handling system and control panel for the x-ray preionized, pulsed avalanche/self-sustained discharge apparatus at UC San Diego.

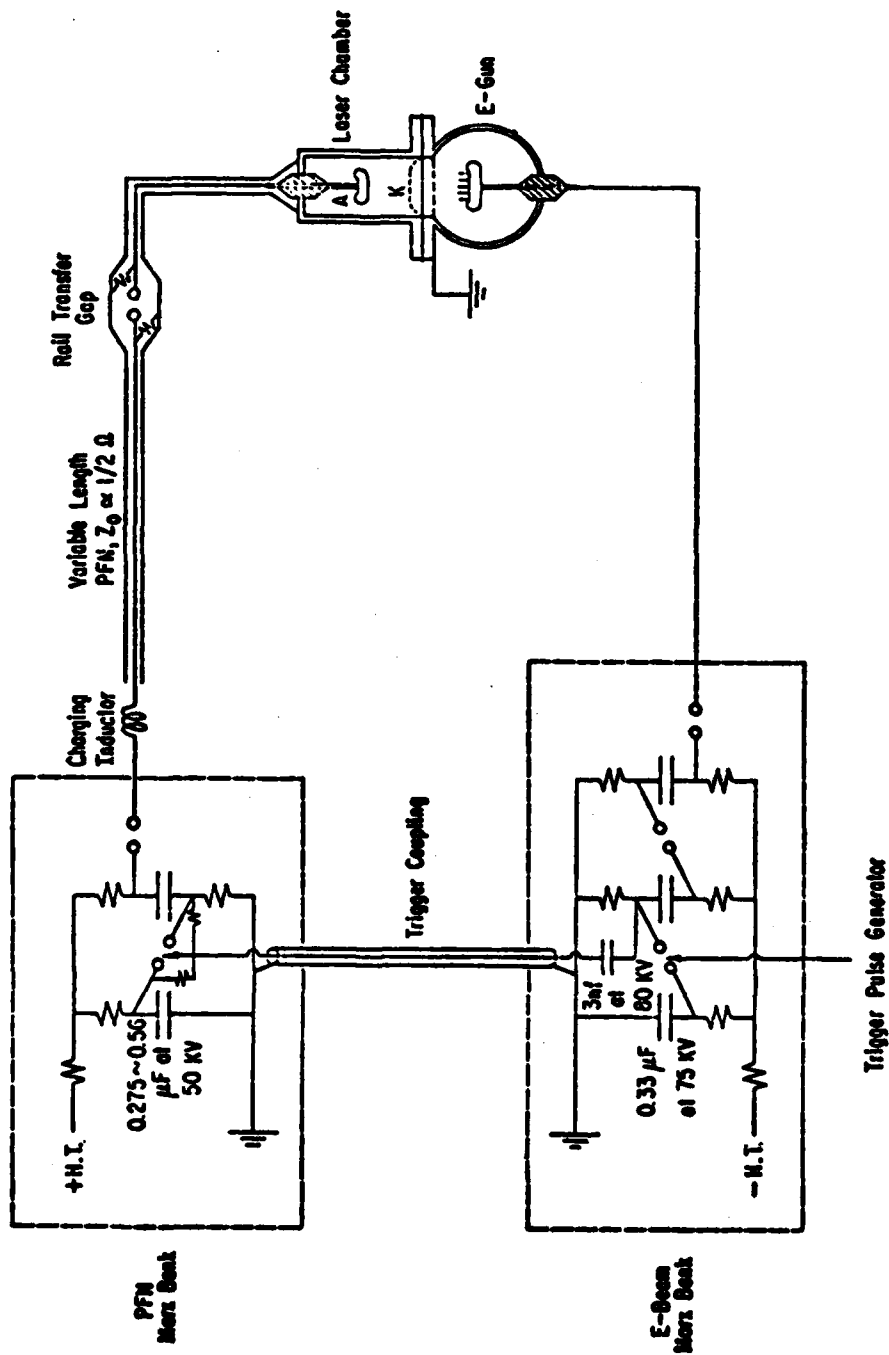


Fig. 6. Schematic diagram showing some details of the electrical driving circuits and actual experimental arrangement for the X-ray preionized, low inductance, transmission-line-driven discharge apparatus illustrated in Figs. 3 and 4.

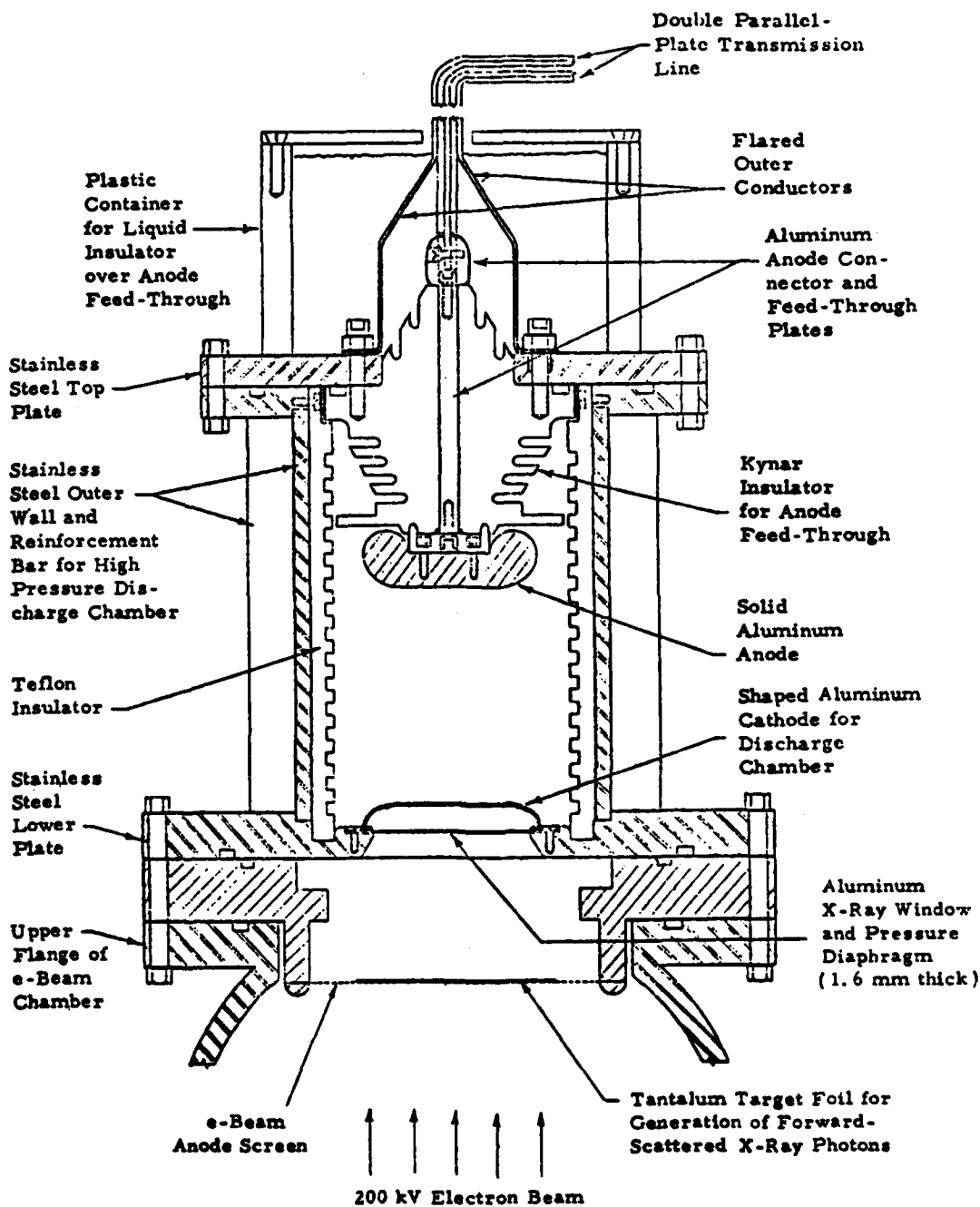


Fig. 7. Cross-sectional drawing of the laser chamber showing some detailed structures of the high voltage insulators, discharge electrodes, and X-ray preionization source. The electrodes are 110 cm long. The discharge volume is adjustable by variation of the gap spacing and effective width of the electrodes.

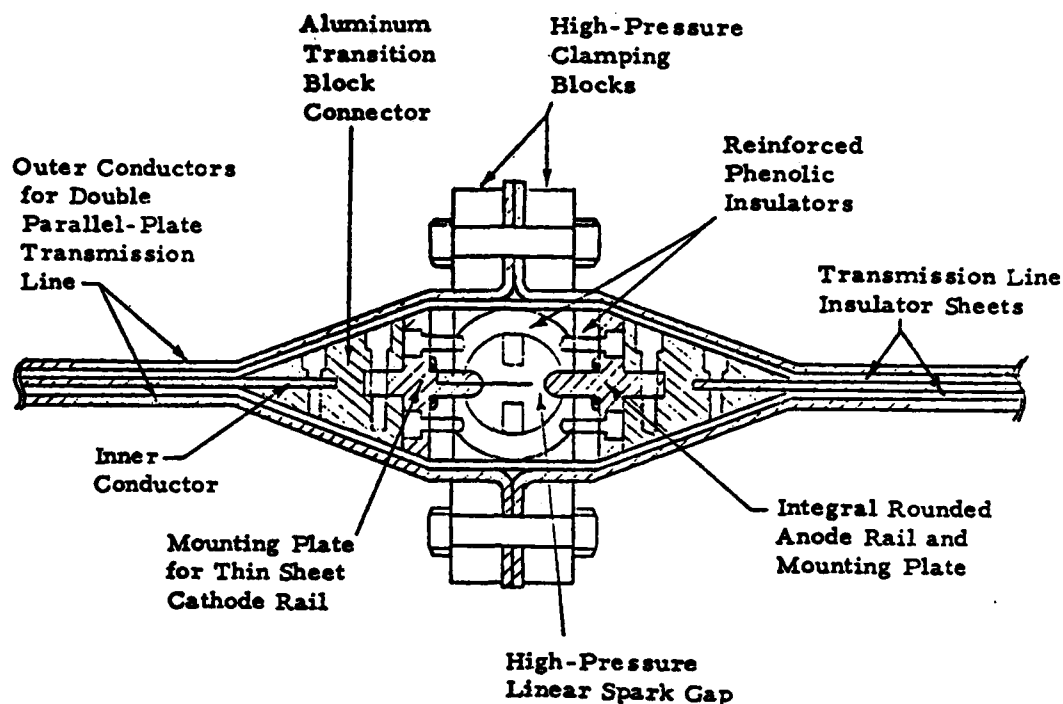


Fig. 8. Cross-sectional drawing of the self-triggered rail gap employed in the discharge circuit for initial voltage isolation and for subsequent rapid transfer of the pulse-charged voltage from the transmission line to the laser chamber. Proper synchronization of the sharp (short rise time) high voltage pulse at the discharge electrodes and the X-ray preionization pulse is essential for homogeneous avalanche formation and stable sustenance of the high pressure discharge.

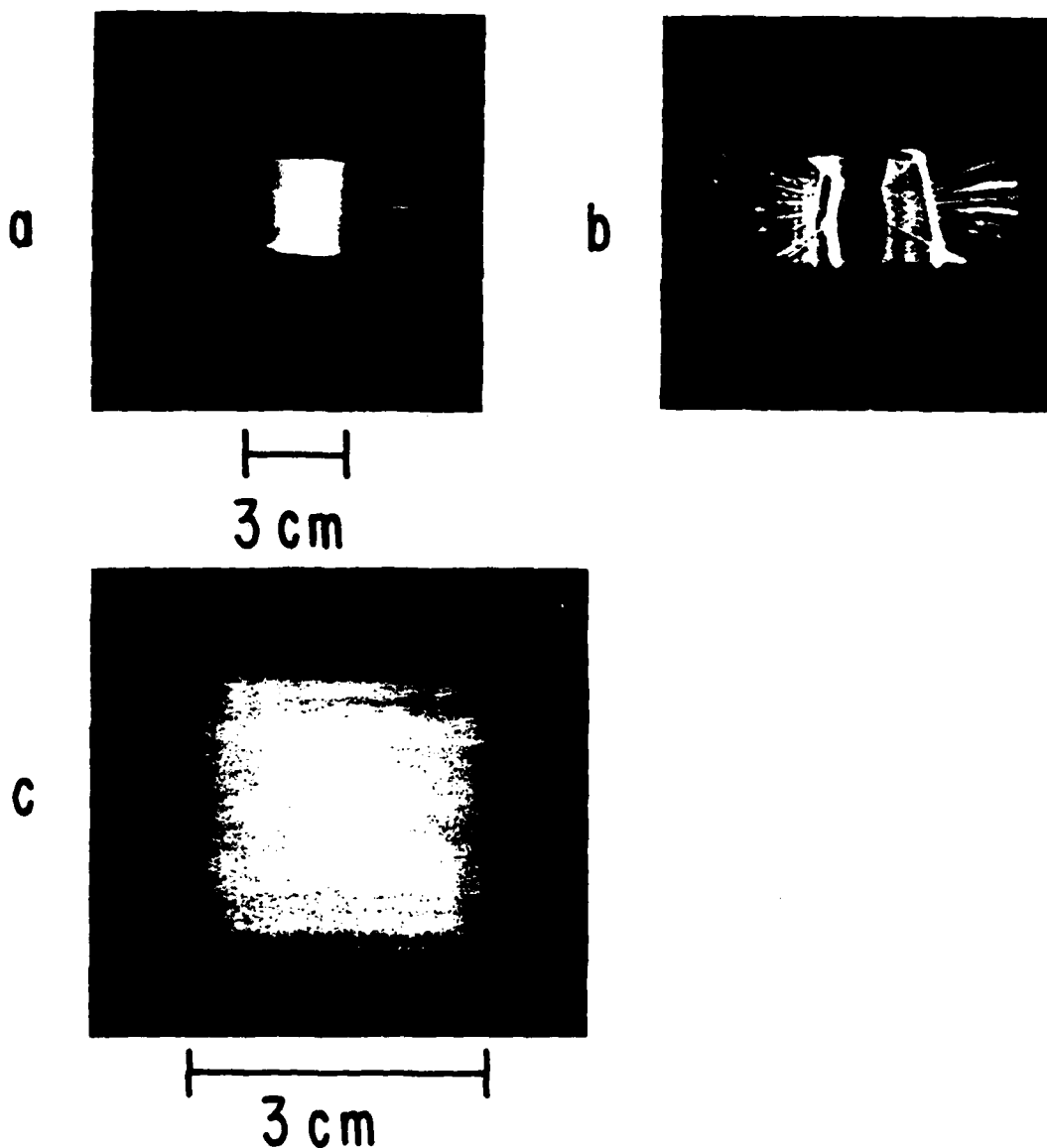


Fig. 9. Top row: Polaroid photographs from open-shutter camera looking directly into the laser chamber through one of the quartz end windows during a discharge in rare gas/halogen mixture showing (a) homogeneous discharge with X-ray preionization; (b) inhomogeneous discharge in the absence of x-ray preionization. Bottom picture: uv burn pattern on Polaroid film target from the output beam of a single pulse, x-ray preionized, rare gas halide excimer laser discharge.

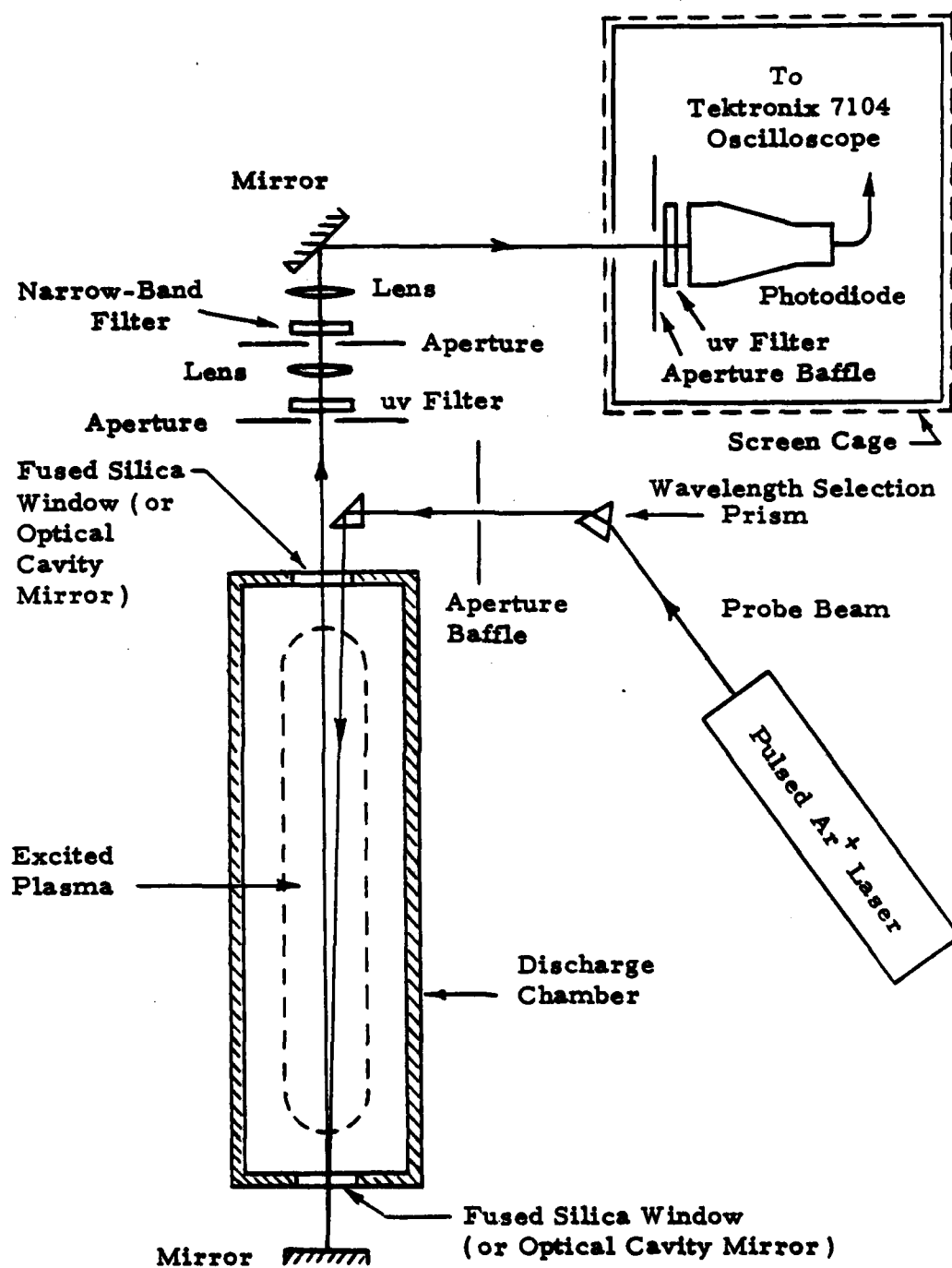


Fig. 10. Schematic diagram showing experimental arrangements for the measurement of spectral absorption and gain at the XeF C - A transition wavelengths with and without trapping of the B - X resonance radiation.

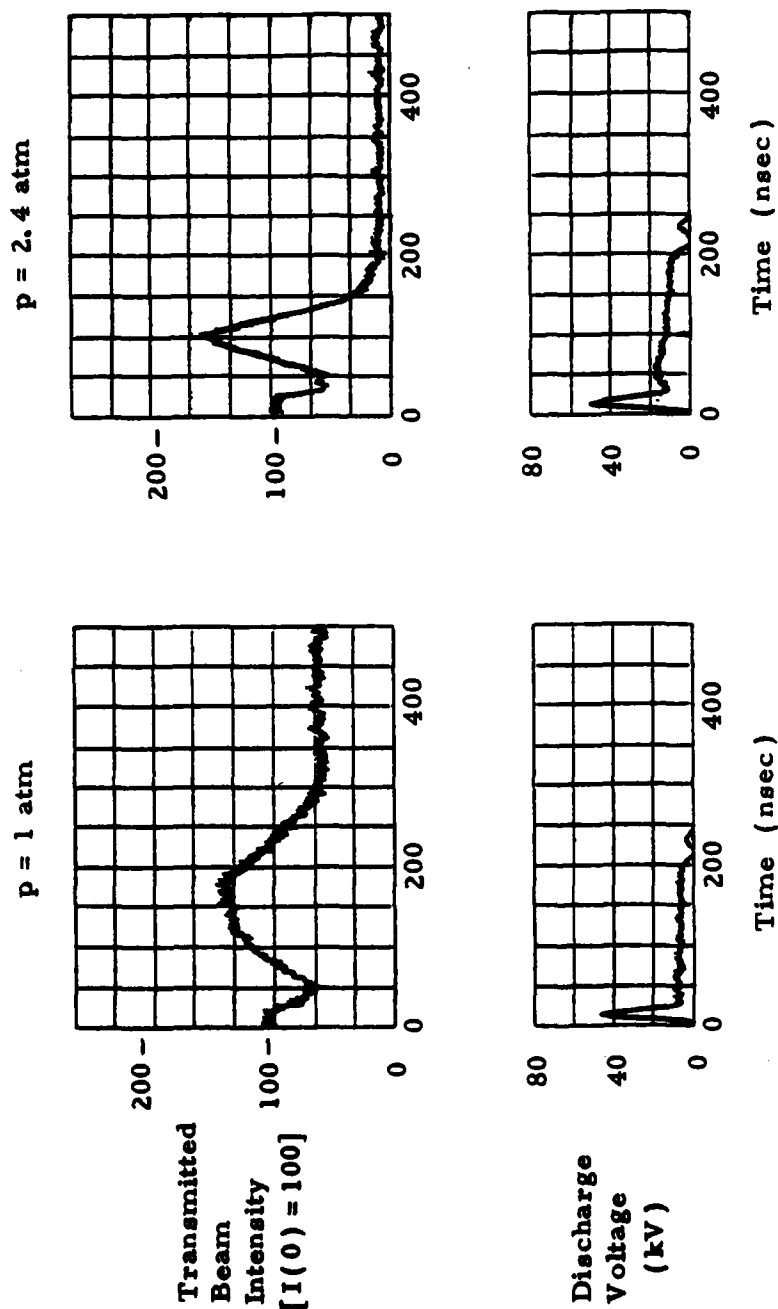


Fig. 11. Typical oscillographic traces of the transmitted beam intensity through the excited plasma (upper traces) and of the discharge voltage (lower traces) observed in the spectral absorption and gain measurements at the XeF C \rightarrow A transition wavelengths in the absence of B \rightarrow X resonance radiation trapping. These are obtained by using only fused silica end windows on the discharge chamber (Fig. 10) in a 200 nsec discharge with a He:Xe:NF₃ = 996:3:1 mixture at two different values of the total gas pressure p . Probe beam wavelength, $\lambda = 487.99 \text{ nm}$.

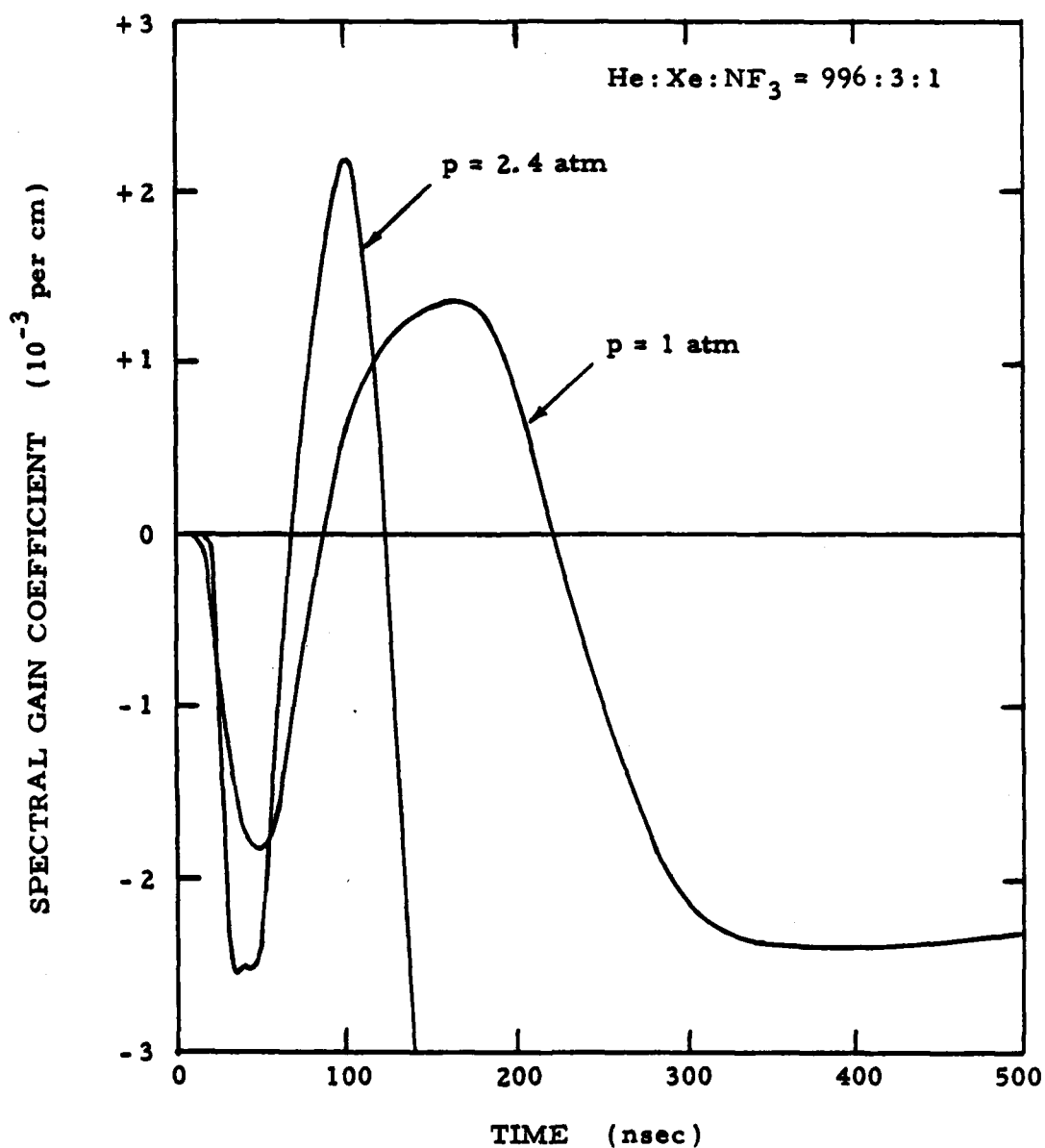


Fig. 12. Typical time variations of the spectral gain coefficient in the absence of XeF B - X resonance radiation trapping observed at two different values of the total gas pressure p in a 200 nsec pulsed avalanche discharge using a He:Xe:Nf₃ = 996:3:1 mixture. These are deduced directly from the smoothed out oscillographic traces shown in Fig. 11 for the transmitted beam intensity at the probe beam wavelength $\lambda = 487.99$ nm and from the known pulse shape of the Ar⁺ laser power output (Fig. 10).

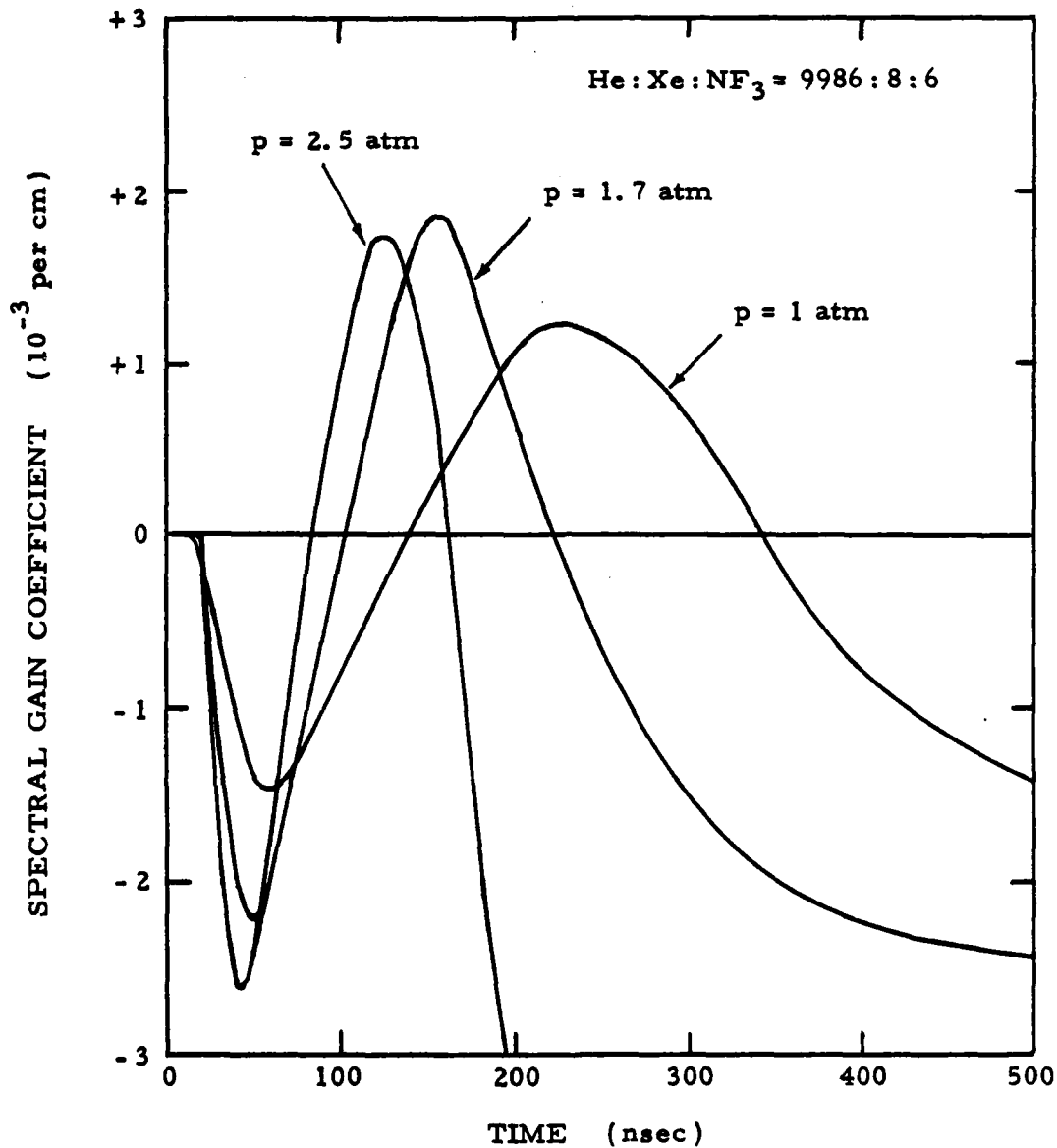


Fig. 13. Time variations of the spectral gain coefficient in the absence of XeF B - X resonance radiation trapping observed at three different values of the total gas pressure p in a 100 nsec pulsed avalanche discharge using a He:Xe:NF₃ = 9986:8:6 mixture. The smoothed out curves represent averaged values deduced from oscillographic traces of the type illustrated in Fig. 11 for the transmitted beam intensity at a fixed wavelength $\lambda = 487.99$ nm, assuming a linear photodiode response.

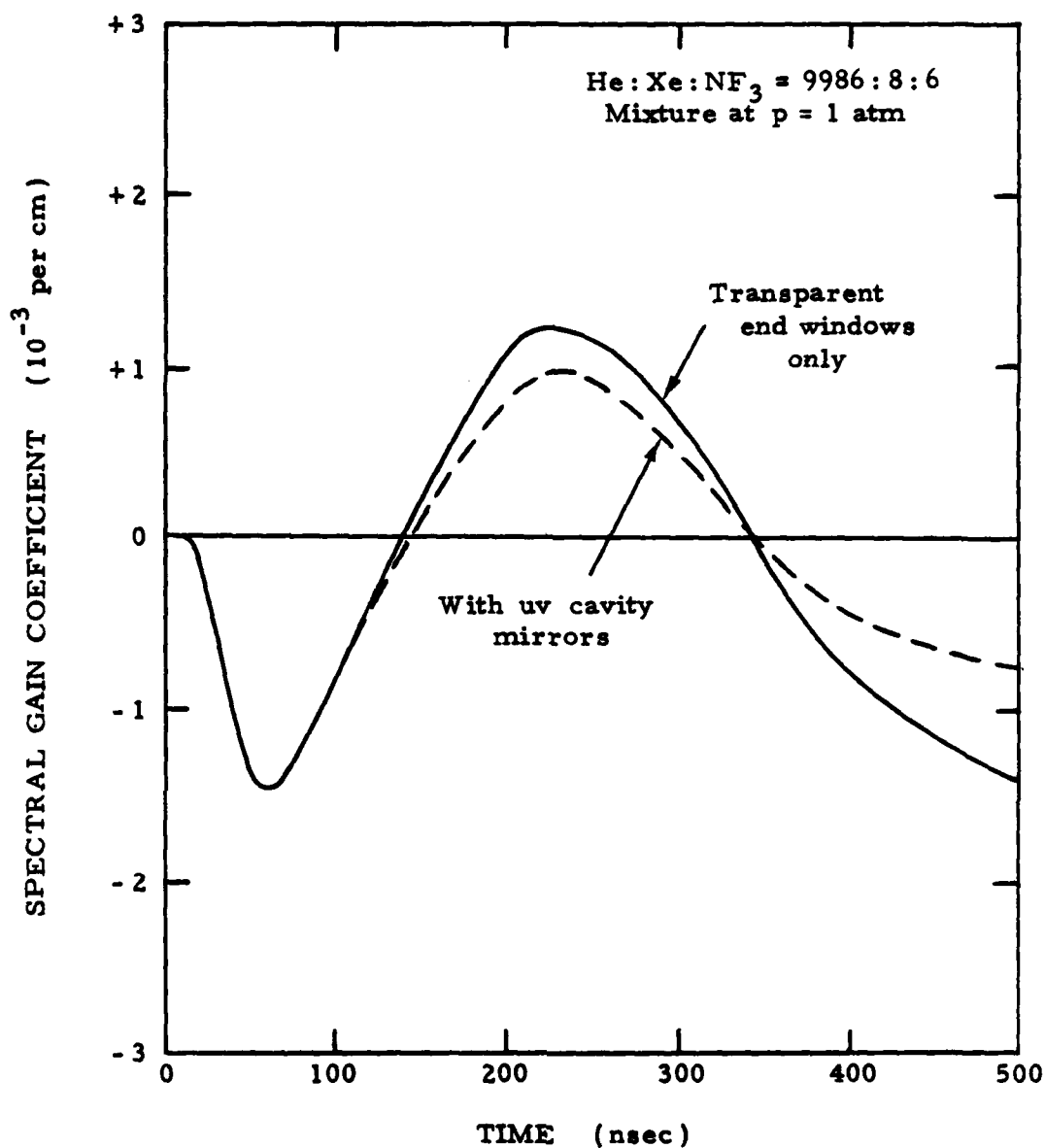


Fig. 14. Comparison of the spectral gain coefficient observed in the 100 nsec pulsed avalanche discharge in the absence (solid curve) and in the presence (dotted curve) of XeF B - X resonance radiation trapping. The solid curve is the same as the one shown in Fig. 13 for $p = 1$ atm. The dotted curve is obtained under the same set of discharge conditions but with the fused silica end windows (Fig. 10) replaced by a pair of pre-aligned optical cavity mirrors of $\sim 98\%$ reflectance at $\lambda = 351$ nm and $\sim 90\%$ transmittance at the probe beam wavelength, $\lambda = 487.99$ nm.

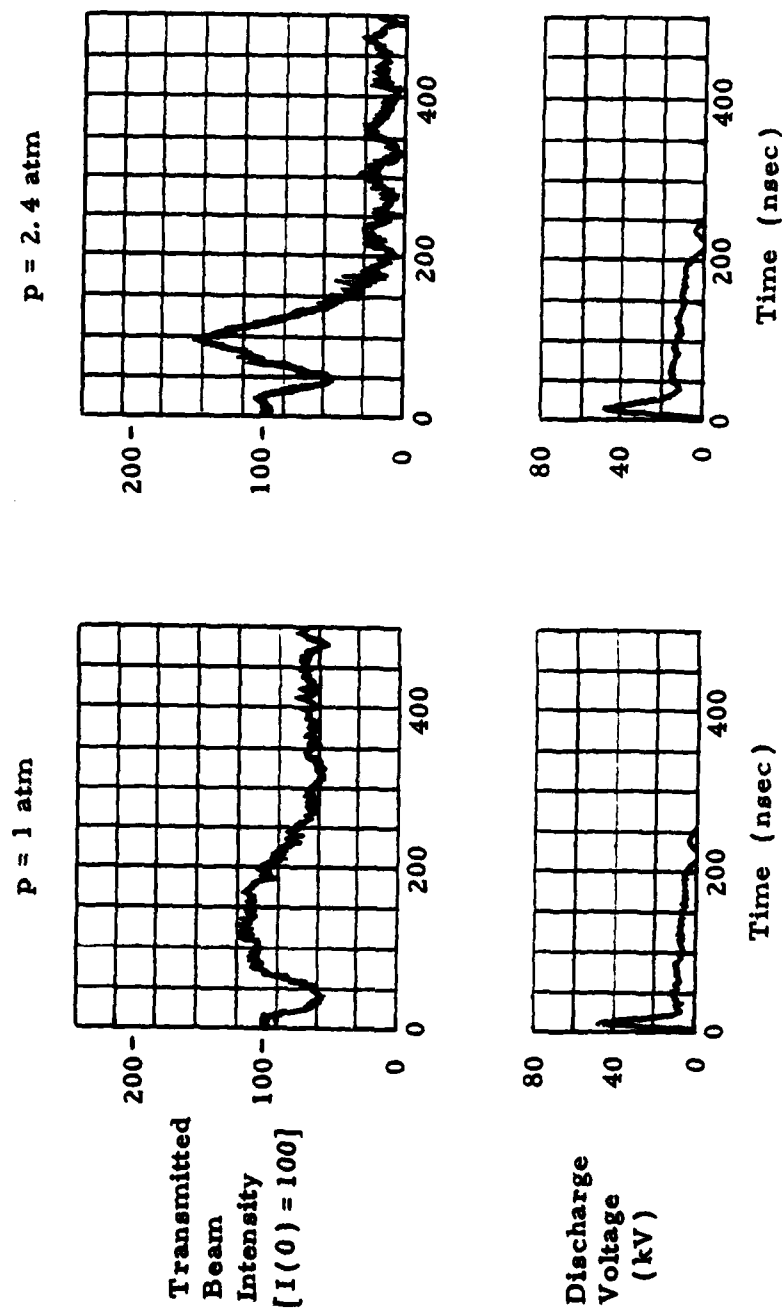


Fig. 15. Typical oscillographic traces of the transmitted beam intensity through the excited plasma (upper traces) and of the discharge voltage (lower traces) observed in the spectral absorption and gain measurements at the XeF C \rightarrow A transition wavelengths in the presence of B \rightarrow X resonance radiation trapping. These are obtained by using dichromatic optical cavity mirrors in place of the fused silica end windows on the discharge chamber (Fig. 10) in a 200 nsec discharge with a He:Xe:NF₃ = 996:3:1 mixture at two different values of the total gas pressure p . Probe beam wavelength, $\lambda = 487.99 \text{ nm}$.

FEED